

## COMMUNICATIONS

**Anomalous charge-transfer behavior in the scattering of hyperthermal  $\text{Br}^+(\text{}^3P_2)$  on Pt(111)**M. Maazouz, P. L. Maazouz, and D. C. Jacobs<sup>a)</sup>*Department of Chemistry and Biochemistry, University of Notre Dame, Notre Dame, Indiana 46556*

(Received 8 August 2002; accepted 23 October 2002)

In contrast to conventional charge-transfer theory, the scattering of state-selected  $\text{Br}^+(\text{}^3P_2)$  on Pt(111) shows a dramatic enhancement in the yield of  $\text{Br}^-(\text{}^1S_0)$  at an impact energy of 26 eV. Coincident with this resonance, the  $\text{Br}^-(\text{}^1S_0)$  product scatters with additional translational energy. The observed scattering behavior is consistent with a collision-induced deformation of the lattice that evolves in phase with the departing projectile. The experimental data demonstrate the strong coupling between the motion of the platinum lattice and the surface electronic states responsible for charge transfer. © 2002 American Institute of Physics. [DOI: 10.1063/1.1529687]

Hyperthermal energy (5–500 eV) ion–surface interactions have gained considerable attention because of their relevance to numerous applications, ranging from plasma processing in the microelectronics industry to the degradation of spacecraft materials in low-earth orbit.<sup>1</sup> Of fundamental interest are the diverse reaction pathways accessible to the ion/surface system when the energy of the collision greatly exceeds that encountered under thermal conditions.<sup>2</sup>

The majority of ion/surface scattering experiments have involved light atomic projectiles striking crystalline targets at keV impact energies.<sup>3</sup> Theoretical models, such as the Anderson–Newns formalism, are often employed to quantitatively treat resonant charge–exchange during scattering.<sup>4</sup> If the projectile’s affinity level becomes resonant with occupied states of the substrate along the inbound trajectory, rapid charge transfer will typically allow the projectile to reach and track its equilibrium charge state. Nevertheless, along the outgoing trajectory, the charge transfer rate diminishes rapidly, and the charge on the projectile eventually becomes “frozen.”<sup>5</sup> For negative ion emergence, a simplified “freezing distance model” predicts that the yield of scattered anions will increase dramatically with increasing exit velocity—in agreement with experiment.<sup>6,7</sup>

Implicit to conventional charge-transfer theory is the simplifying approximation that the surface electronic structure is not significantly perturbed by the impulsive collision. This assumption is justified in the case where a light projectile strikes a heavy target atom. Under these conditions, the scattered particle leaves rapidly before the lattice has time to respond to the impact. Furthermore, because the majority of scattering experiments have involved oblique angles of incidence and detection, the projectile’s final charge state is thought to be determined after the particle has traversed laterally from the original impact site to an unperturbed region of the surface. Notwithstanding, the displacement of surface

atoms, such as that created in a violent collision, may locally perturb the electronic structure of the solid target.<sup>8,9</sup> If the projectile departs along the surface normal and moves slowly relative to the time scale of the lattice distortion, the charge-transfer dynamics can be significantly affected by the transient surface deformation.

With the support of classical trajectory simulations, some groups have examined the role of collision-induced surface deformations in the hyperthermal energy scattering of heavy atomic projectiles on well-characterized surfaces. Amirav *et al.* proposed a multiple-collision model in which a 1–10 eV Xe atom struck a target atom, only to have the target atom return and collide with the Xe projectile a second time.<sup>10</sup> A similar mechanism was proposed by Sosolic and Cooper in the scattering of 10–250 eV  $\text{Rb}^+$  on Cu(001).<sup>11</sup> Keller *et al.* investigated the neutralization of  $\text{Na}^+$  on Cu(001) at 7.5 and 50 eV.<sup>12</sup> They proposed that the neutralization probability depended significantly on the impact site and the ensuing trajectory; the most complex trajectories suffered large energy losses and deformed the surface locally; these trajectories had charge-transfer probabilities that were dramatically higher than the less obtrusive, single-scattering trajectories.

In the present study, experiments are performed in which state-selected, hyperthermal energy  $\text{Br}^+(\text{}^3P_2)$  is targeted at a well-characterized Pt(111) surface. The chosen scattering conditions are ideal for exploring how a transient deformation of the surface significantly alters charge-exchange in ion–solid collisions.

The experimental configuration is described in detail elsewhere; thus, only a brief description will be given here.<sup>13</sup> Prior to the experiment, the platinum surface is prepared by repeated cycles of  $\text{Ar}^+$  sputtering (500 eV, 6  $\mu\text{A}$  ion beam directed 60° from the surface normal;  $T_s=300$  K) and annealing ( $T_s=1175$  K).<sup>14</sup> A doubly differentially-pumped, pulsed molecular beam delivers  $\text{Br}_2(\text{g})$  into the ultrahigh vacuum (UHV) scattering chamber ( $P<4\times 10^{-10}$  Torr). Single-color ultraviolet photodissociation of  $\text{Br}_2$ , followed

<sup>a)</sup> Author to whom correspondence should be addressed. Electronic mail: jacobs.2@nd.edu; Fax: (574) 631-6652.

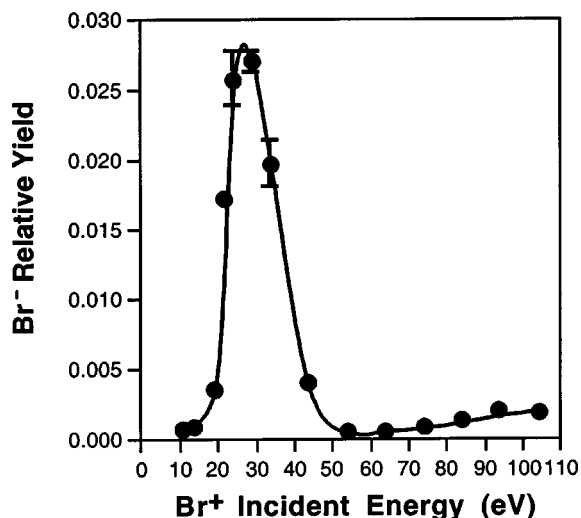


FIG. 1. Relative yield of scattered  $\text{Br}^-(^1S_0)$  product vs kinetic energy for  $\text{Br}^+(^3P_2)$  incident on Pt(111). The curve is drawn to guide the eye.

by 2+1 resonance-enhanced multiphoton ionization (REMPI) at  $\lambda = 277.19$  nm, produces  $\text{Br}^+$  in the  $^3P_2$  electronic state (84% population).<sup>15,16</sup> The state-selected  $\text{Br}^+(^3P_2)$  ions are extracted, accelerated, mass-selected, and finally decelerated to 10–105 eV (1 eV FWHM) before colliding with the clean Pt(111) surface. The pulsed ion beam typically delivers  $\sim 10^2$   $\text{Br}^+(^3P_2)$  ions per laser shot (20-Hz repetition rate), corresponding to a time-integrated exposure rate of less than  $10^{-7}$  Langmuirs per hour. Consequently, it is reasonable to assert that the Pt(111) surface is not significantly modified by the impinging  $\text{Br}^+(^3P_2)$  ions during the course of the experiment.

The incident and scattered ions are monitored with a novel ion-imaging detector, specifically designed to afford mass-, angle-, and velocity-resolution with near single-ion detection efficiency.<sup>17</sup> The spatial distribution of ions is recorded on a CCD camera at a particular instant in time. The digitized image reflects the ions' two-dimensional velocity distribution in the scattering plane. The imaging detector is positioned along the ion-beam axis, collinear with the surface normal. The solid angle over which ions are collected is  $\pm 28^\circ$  (in-plane) and  $\pm 7^\circ$  (out-of-plane) relative to the surface normal. This normal-incidence/normal-detection scattering geometry enables the detector to collect incident  $\text{Br}^+$  ions and scattered ionic products on alternating laser shots. In this way, a relative ion yield is calculated from the number of collected product ions, integrated over all velocities within the acceptance angle of the detector, divided by the number of incident ions.

Across the 10–105 eV range of impact energies, less than  $10^{-5}$  of the incident  $\text{Br}^+(^3P_2)$  ions scatter with their positive charge intact. Facile neutralization along the inbound trajectory is followed, to a lesser extent, by a second electron capture to produce scattered  $\text{Br}^-$ . For negative ion formation on metal surfaces, there is no evidence to suggest that the two electron-transfer events are concerted or even correlated.<sup>18</sup> Because only  $\text{Br}^-$  in its ground electronic state ( $^1S_0$ ) is stable against autodetachment, the scattering experi-

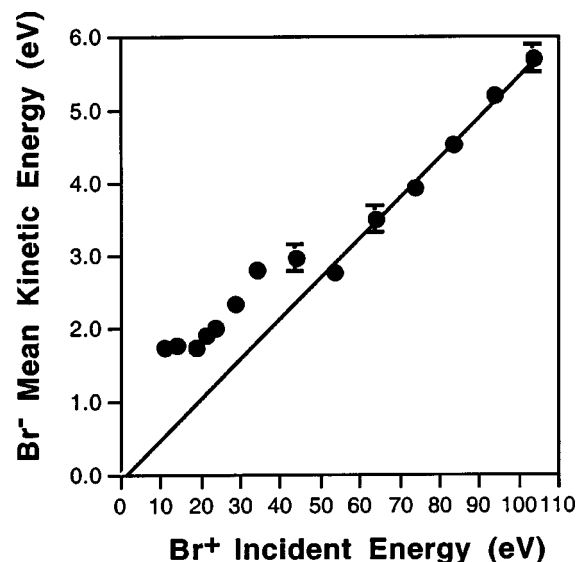


FIG. 2. Mean translational energy of scattered  $\text{Br}^-(^1S_0)$  product as a function of kinetic energy of incident  $\text{Br}^+(^3P_2)$ . A linear relationship is observed for incident energies greater than 55 eV.

ment resolves the state-to-state transformation of  $\text{Br}^+(^3P_2)$  to  $\text{Br}^-(^1S_0)$  on Pt(111) at  $T_s = 300$  K.

Figure 1 demonstrates the extreme sensitivity of  $\text{Br}^-(^1S_0)$  emergence to the kinetic energy of incident  $\text{Br}^+(^3P_2)$ . The most intriguing feature is the sharp resonance near 26 eV. At the peak of the resonance, the relative yield of  $\text{Br}^-(^1S_0)$  products equals 2.8% of the incident  $\text{Br}^+(^3P_2)$  reactants. From the recorded angular distribution of the scattered  $\text{Br}^-(^1S_0)$  signal, it is predicted that only 40% of the emergent product ions are collected within the solid angle element of the detector. Consequently, the absolute yield of  $\text{Br}^-(^1S_0)$ , integrated over all scattering angles and velocities, is estimated to be 7% of the incident 26 eV  $\text{Br}^+(^3P_2)$  ions. Surprisingly, the  $\text{Br}^-(^1S_0)$  yield drops by an order of magnitude when the kinetic energy of incident  $\text{Br}^+(^3P_2)$  is increased by only 20 eV. Further, the  $\text{Br}^-(^1S_0)$  yield gradually increases when the incident energy exceeds 55 eV.

Figure 2 shows the dependence of the scattered  $\text{Br}^-(^1S_0)$  translational energy on the incident  $\text{Br}^+(^3P_2)$  energy. Again, two different scattering regimes appear in the data. For incident energies greater than 55 eV, the mean translational energy of scattered  $\text{Br}^-(^1S_0)$  is 5.4% of the  $\text{Br}^+(^3P_2)$  kinetic energy. However, for incident energies below 55 eV, the final kinetic energy of  $\text{Br}^-(^1S_0)$  is augmented by as much as 1 eV when compared to the linear trend found for impact energies above 55 eV. This enhancement in the scattered  $\text{Br}^-(^1S_0)$  kinetic energy occurs across the same range of incident energies as the resonance appearing in Fig. 1.

The connection between the data in Figs. 1 and 2 is most revealing. For example, a comparison of the scattering behavior for 34 and 54 eV  $\text{Br}^+(^3P_2)$  indicates that in both cases, the scattered  $\text{Br}^-(^1S_0)$  products leave the surface with a mean energy of 2.8 eV. If the final charge-state depends only on the outgoing velocity, then both scattering conditions should produce a similar anion yield. Yet, the relative yield for 34 eV  $\text{Br}^+(^3P_2)$  is a factor of thirty larger than the rela-

tive yield for 54 eV Br<sup>+</sup> (<sup>3</sup>P<sub>2</sub>). Alternatively, if one judged that the incident velocity should be important in determining the degree of surface penetration and hence the probability for electron capture, then conventional charge-transfer wisdom might lead one to predict incorrectly that the faster projectile should exhibit the greater anion yield. The experimental data underscore the importance of considering the entire scattering trajectory when examining charge-transfer behavior.

The drop in the Br<sup>-</sup> (<sup>1</sup>S<sub>0</sub>) yield above 26 eV could be attributed to the onset of implantation. However, the threshold for implantation on the close-packed Pt(111) surface is expected to be higher than the penetration threshold for Kr<sup>+</sup> impinging on graphite [48 eV] or on W(100) [100 eV]; furthermore, the precipitous drop in the anion yield is uncharacteristic of the rate at which implantation increases with impact energy.<sup>19,20</sup>

A more plausible explanation for the resonance feature focuses on the temporal response of the lattice to the impulsive collision. A 26-eV incident Br<sup>+</sup> (<sup>3</sup>P<sub>2</sub>) projectile rapidly dumps approximately 27 eV of translational and electronic energy into a localized region of the surface.<sup>21</sup> The impulse travels as a shock wave into the lattice and is eventually dissipated.<sup>22</sup> Preliminary classical trajectory calculations suggest that on the time scale of the collision (~200 fs), the near-surface region is transiently distorted into an indentation followed by a protrusion. This lattice deformation can significantly perturb the local electronic structure of the surface proximate to the point of impact.<sup>8,9</sup>

Local effects have been shown to strongly influence charge-transfer dynamics.<sup>23,24</sup> Taylor and Nordlander demonstrated that the level-width (a measure of the tunneling rate) for electron transfer is significantly modulated by the lateral position of a Li projectile atom above a corrugated Al(001) surface.<sup>25</sup> Silva *et al.* modeled the electron attachment rate for atomic hydrogen and fluorine projectiles striking a vacancy site on Al(111).<sup>26</sup> They reported that the electron is repelled by the vacancy, thus destabilizing the affinity level near the vacancy site relative to a defect-free region of the surface. Additionally, the investigators noted that the level-width is significantly reduced proximate to the vacancy site. In contrast, the same authors calculated that an Al adatom on the Al(111) surface qualitatively exhibits the opposite effect as that calculated for a vacancy site.<sup>27</sup> In the experiments of Keller *et al.*, it was noted that Na projectiles scattering from Cu(001) had neutralization probabilities differing by a factor of seven, depending on the type of surface collision.<sup>12</sup> The Cornell group argued that the trajectory-dependent charge-transfer probability could be traced to the way in which the lattice is deformed by the collision. By employing a static dipole approximation to simulate the collision-induced vacancy site, the authors' charge-transfer model achieved qualitative agreement with the data.

The localized perturbations to charge transfer cited above are significant; however, the investigators all treated the surface defect statically, i.e., the lattice was assumed to be rigid. In the present experiments, the collision-induced deformation of the surface is transient and evolves on the time scale of the projectile's interaction with the surface. The

velocity with which scattered Br<sup>-</sup> (<sup>1</sup>S<sub>0</sub>) asymptotically departs from the Pt(111) surface is 1 Å per 45 fs, when Br<sup>+</sup> (<sup>3</sup>P<sub>2</sub>) is incident at 26 eV. Considering that charge transfer will occur as long as the particle is within a few Å of the surface, it is reasonable to expect that the ion/surface interaction time will extend over a period of a couple hundred fs after the point of impact. This is ample time for the lattice deformation to undergo a partial oscillation, wherein the escape trajectory of the projectile is synchronously phased with the large-amplitude motion of the surface atoms.

Electron attachment preferentially involves electrons propagating along the surface normal, because the tunneling barrier between the surface and the projectile is narrowest in this case.<sup>28,29</sup> Yet the electronic structure of static Pt(111) features a projected band gap at the  $\bar{\Gamma}$ -point extending from the Fermi level to the vacuum level.<sup>30</sup> The projected band gap arises from the void in **k**-space of wave functions carrying zero-momentum parallel to the surface.<sup>31</sup> A distortion of the lattice will locally perturb the electronic states near the band gap region, especially the *sp*-derived surface resonance lying 0.2 eV below the Fermi level.<sup>32</sup> Because the transient deformation of the lattice occurs on a time scale that is slow compared to electron reorganization, the surface electron occupancies are predominantly expected to adiabatically track the nuclear motion. Nevertheless, nonadiabaticity will generate electron-hole pairs proximal to the impact site. Hot electrons (with energies above the Fermi level) excited by the violent collision may enhance electron capture by efficiently coupling with the projectile's affinity level. It is expected that the lifetime of a hot electron on Pt(111) will exceed that measured for Cu(111) [20–35 fs], because the dominant *d*- versus *s*-character of Pt contributes to a greater density of states near the Fermi level.<sup>33</sup>

The resonance feature in Fig. 1 is moderated by the second electron transfer event and not the first, because neutralization is virtually complete in this system. We postulate that the anomalous enhancement in the Br<sup>-</sup> (<sup>1</sup>S<sub>0</sub>) yield for 26 eV incident Br<sup>+</sup> (<sup>3</sup>P<sub>2</sub>) is caused by a localized perturbation (to the electronic structure, state occupancies, and charge-transfer couplings) induced by the collisional distortion of the lattice. At the peak of the resonance, the transient surface deformation (and its associated electronic perturbation) occurs at an optimal phase relative to the projectile's departure from the surface. In addition to considering factors affecting the electron capture process, an equally important issue in Br<sup>-</sup> emergence concerns the potential transfer of the electron back to the surface along the outgoing trajectory. Electron loss is energetically favored, because the surface work function exceeds the electron affinity of isolated Br by 2.6 eV. Nonetheless, the projected band gap for Pt(111) can impede electron loss significantly, if there are no resonant states in the metal to couple with the atom's affinity level.<sup>29</sup> Once again, the synchronization of the lattice deformation with the projectile's exit trajectory is critical to fully treating the time-dependent couplings responsible for electron loss.

The Br/Pt(111) system exhibits an unprecedented resonance in the electron-transfer dynamics. The conditions leading to this phenomenon are critically sensitive to the timing with which the Br projectile scatters from the surface and the

transient response of the lattice to the impulsive collision. It is worth speculating on why a resonance appears in this study when it has not been observed in any other. First, the unconventional experimental configuration (normal incidence/normal detection) employed here is ideally suited for probing local effects in scattering. Second, synchronizing the lattice distortion to the motion of the scattered particle requires that the projectile be relatively massive and that it strikes the surface at a low velocity (8 km/s or 0.004 au in the present case). Third, charge transfer is most sensitive to the scattering conditions in systems where the affinity level crosses the Fermi level near the classical turning point of the trajectory. Clearly, realistic theoretical simulations are needed to fully characterize the mechanism leading to the resonance phenomenon. To further explore the generality of the resonance, more experiments are warranted on various metal surfaces, where the electronic structure, acoustic properties, crystallographic orientation and surface temperature can be systematically varied. Furthermore, it remains to be seen whether this intriguing phenomenon persists for other projectiles—both molecular and atomic.

Support from the National Science Foundation (CHE99-86374) is gratefully acknowledged.

- <sup>1</sup>D. C. Jacobs, in *Chemical Dynamics in Extreme Environments*, edited by R. Dressler (World Scientific, River Edge, NJ, 2001), p. 349.
- <sup>2</sup>D. C. Jacobs, *Annu. Rev. Phys. Chem.* **53**, 379 (2002).
- <sup>3</sup>H. Winter, *Phys. Rep.* **367**, 387 (2002).
- <sup>4</sup>J. Los and J. J. C. Geerlings, *Phys. Rep.* **190**, 133 (1990).
- <sup>5</sup>G. A. Kimmel and B. H. Cooper, *Phys. Rev. B* **48**, 12164 (1993).
- <sup>6</sup>J. R. Morris, G. Kim, T. L. O. Barstis, R. Mitra, and D. C. Jacobs, *J. Chem. Phys.* **107**, 6448 (1997).
- <sup>7</sup>A. Bekkerman, B. Tsipinyuk, and E. Kolodney, *J. Chem. Phys.* **116**, 10447 (2002).
- <sup>8</sup>R. E. Walkup and Ph. Avouris, *Phys. Rev. B* **39**, 5504 (1989).
- <sup>9</sup>K. W. Sulston and S. G. Davison, *Surf. Sci.* **261**, 335 (1992).
- <sup>10</sup>A. Amirav, M. J. Cardillo, P. L. Trevor, C. Lim, and J. C. Tully, *J. Chem. Phys.* **87**, 1796 (1987).
- <sup>11</sup>C. E. Sosolik and B. H. Cooper, *Nucl. Instrum. Methods Phys. Res. B* **182**, 167 (2001).
- <sup>12</sup>C. A. Keller, C. A. Dirubio, G. A. Kimmel, and B. H. Cooper, *Phys. Rev. Lett.* **75**, 1654 (1995).
- <sup>13</sup>J. S. Martin, J. M. Greeley, J. R. Morris, B. T. Feranchak, and D. C. Jacobs, *J. Chem. Phys.* **100**, 6791 (1994).
- <sup>14</sup>K. Christmann, G. Ertl, and T. Pignet, *Surf. Sci.* **54**, 365 (1976).
- <sup>15</sup>Y. S. Kim, Y.-J. Jung, W. Kang, and K.-H. Jung, *Bull. Korean Chem. Soc.* **23**, 189 (2002).
- <sup>16</sup>B. G. Koenders, G. J. Kuik, K. E. Drabe, and C. A. De Lange, *Chem. Phys. Lett.* **147**, 310 (1988).
- <sup>17</sup>M. Maazouz, J. R. Morris, and D. C. Jacobs, in *Imaging in Chemical Dynamics*, edited by A. Suits and R. Continetti (American Chemical Society, Washington, D.C., 2001), pp. 139–150.
- <sup>18</sup>P. Roncin, A. G. Borisov, H. Khemliche, A. Momeni, A. Mertens, and H. Winter, *Phys. Rev. Lett.* **89**, 043201 (2002).
- <sup>19</sup>D. Marton, K. J. Boyd, T. Lytle, and J. W. Rabalais, *Phys. Rev. B* **48**, 6757 (1993).
- <sup>20</sup>E. V. Kornelsen and M. K. Sinha, *J. Appl. Phys.* **39**, 4546 (1968).
- <sup>21</sup>When 26 eV Br<sup>+</sup>(<sup>3</sup>P<sub>2</sub>) is incident on Pt(111), the scattered Br<sup>-</sup>(<sup>1</sup>S<sub>0</sub>) product leaves with only 2.1 eV kinetic energy. The asymptotic exoergicity of the double electron-transfer is calculated from the ionization potential (11.81 eV) and the electron affinity (3.36 eV) of Br minus twice the work function (5.95 eV) of Pt(111). Consequently, ~27 eV is deposited as both electronic and vibrational excitations in the lattice.
- <sup>22</sup>Y. Zeiri and R. R. Lucchese, *J. Chem. Phys.* **94**, 4055 (1991).
- <sup>23</sup>K. A. H. German, C. B. Weare, P. R. Varekamp, J. N. Andersen, and J. A. Yarmoff, *Phys. Rev. Lett.* **70**, 3510 (1993).
- <sup>24</sup>J. P. Gauyacq and A. G. Borisov, *J. Phys.: Condens. Matter* **10**, 6585 (1998).
- <sup>25</sup>M. Taylor and P. Nordlander, *Phys. Rev. B* **64**, 115422 (2001).
- <sup>26</sup>J. A. M. C. Silva, A. G. Borisov, J. P. Gauyacq, P. Nordlander, D. Teillet-Billy, and J. Wolfgang, *Nucl. Instrum. Methods Phys. Res. B* **157**, 55 (1999).
- <sup>27</sup>J. A. M. C. Silva, J. Wolfgang, A. G. Borisov, J. P. Gauyacq, P. Nordlander, and D. Teillet-Billy, *Surf. Sci.* **506**, 145 (2002).
- <sup>28</sup>M. Maazouz, A. G. Borisov, V. A. Esaulov, J. P. Gauyacq, L. Guillemot, S. Lacombe, and D. Teillet-Billy, *Phys. Rev. B* **55**, 13869 (1997).
- <sup>29</sup>A. G. Borisov, J. P. Gauyacq, A. K. Kazansky, E. V. Chulkov, V. M. Silkin, and P. M. Echenique, *Phys. Rev. Lett.* **86**, 488 (2001).
- <sup>30</sup>S. Link, H. A. Dürr, and W. Eberhardt, *Appl. Phys. A: Solids Surf.* **71**, 525 (2000).
- <sup>31</sup>D. Wei, K. E. Smith, and S. D. Kevan, *Phys. Rev. B* **45**, 3652 (1992).
- <sup>32</sup>E. Bertel, *Surf. Sci.* **367**, L61 (1996).
- <sup>33</sup>S. Ogawa, H. Nagano, and H. Petek, *Phys. Rev. B* **55**, 10869 (1997).